Sensors & Actuators: B. Chemical 347 (2021) 130602

Contents lists available at ScienceDirect

Sensors and Actuators: B. Chemical

journal homepage: www.elsevier.com/locate/snb

Durable and flexible Ag-nanowire-embedded PDMS films for the recyclable swabbing detection of malachite green residue in fruits and fingerprints

Juanjuan Luo [a], Zekai Wang [a], Yun Li [b], Changding Wang [a], Jiefang Sun [c], Weichun Ye [a,*], Xiaolong Wang [d,*], Bing Shao [c,*]

[a] State Key Laboratory of Applied Organic Chemistry and Department of Chemistry, Lanzhou University, Lanzhou 730000, China
[b] Lanzhou Institutes for Food and Drug Control, Lanzhou 730050, China
[c] Beijing Key Laboratory of Diagnostic and Traceability Technologies for Food Poisoning, Beijing Center for Disease Prevention and Control, Beijing 10013, China
[d] State Key Laboratory of Solid Lubrication, Lanzhou Institute of Chemical Physics, Chinese Academy of Sciences, Lanzhou 730000, China

ARTICLE INFO

Keywords:
Surface-enhanced Raman scattering
Ag NWs@PDMS film
Portable detection
Malachite green residue

ABSTRACT

Swab sampling for the trace surface-enhanced Raman scattering (SERS) analysis of an aromatic dye (e.g., malachite green, MG) residue in fruits as well as fingerprints is promising due to its practical utility and efficiency in food security and forensic science. However, the durability and recyclability of the SERS substrates pose an enormous challenge. In this study, a novel flexible film was constructed by embedding a commercial Ag nanowire suspension into a polydimethylsiloxane film (Ag NWs@PDMS), which simultaneously exhibits SERS activity, durability and recyclability. High SERS performance was still maintained, even against 20 times stretchability, corrosion by HNO_3, destruction by ultrasonication and a broad working temperature of −20 ℃ to 80 ℃. Excellent recyclability for MG sensing was achieved in ten cycles. Ag NWs@PDMS was successfully used for the quantitative detection of MG in juices of fruits (such as apple and pear) by drop dripping, with a limit of detection of 10 nM and good anti-interference. Meanwhile, the sensitive detection of the MG residue (only 3 ng/cm^2) on fruits was enabled by the on-site surface swabbing by recycling for five cycles. Portable detection of the MG residue was further achieved from the 10th fingerprint after successively touching a dye drop onto the functional film combined with a portable Raman spectrometer.

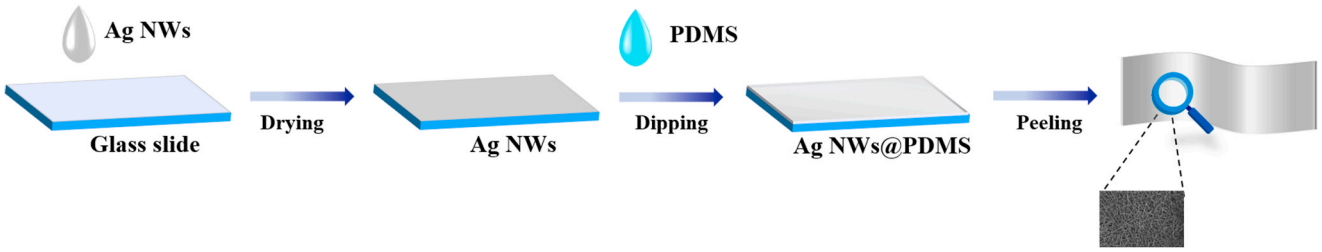
1. Introduction

Malachite green (MG) is one of the important synthetic dyes that has been widely used in dyeing industries for more than 50 years. In addition, it is typically used in consumable products due to its potent antifungal, antibacterial, and antiparasitic activities [1]. Unfortunately, MG can cause teratogenic, carcinogenic, and mutagenic effects against fungal and parasitic infections in humans and animals [2,3]. Owing to these serious side effects, MG is defined as an illegal fungicide, and its use is restricted or prohibited worldwide. Furthermore, aromatic dyes also have been employed for crime tracking via latent fingerprint identification [4,5]. Thus far, conventional analytical techniques have been successfully employed for the sensitive detection of MG, including high-performance liquid chromatography [6], liquid chromatography–tandem mass spectrometry [7], enzyme-linked immunosorbent assay [8], and fluorescence spectroscopy [9]. However, these techniques usually require a complicated pretreatment process and expensive equipment, and they are time consuming, thereby limiting their applications. Therefore, owing to the practicality and efficiency, surface-swabbing contamination analysis for monitoring the MG residues in fruits and fingerprints demonstrates promise [10].

Surface-enhanced Raman spectroscopy (SERS) is recognized as one of the most promising and versatile analytical tools as it is a non-destructive, a rapid, and an ultra-sensitive technique, and it permits real-time analysis and provides molecular information [11]. In the past decades, SERS has been widely applied in environmental monitoring, food safety and forensic science [12,13]. According to the SERS enhancement mechanism, silver is considered as the best SERS material with a strong signal response [14]. Furthermore, fabricating a suitable Ag-based SERS substrate is a key factor to improve the SERS performance. In most cases, silicon and glass sheets are selected as solid supports for various Ag nanostructures; however, their rigid and brittle properties may be inconvenient for actual applications. By contrast, flexible SERS substrates are more favorable for the detection of surface

* Corresponding authors.
E-mail addresses: yewch@lzu.edu.cn (W. Ye), wangxl@licp.cas.cn (X. Wang), shaobingch@sina.com (B. Shao).

https://doi.org/10.1016/j.snb.2021.130602
Received 26 April 2021; Received in revised form 8 August 2021; Accepted 9 August 2021
Available online 12 August 2021
0925-4005/© 2021 Elsevier B.V. All rights reserved.



Scheme 1. Schematic of the fabrication of the Ag NWs@PDMS film.

contamination residues, where the residues can be directly collected by swabbing an irregular or a rough surface with minimal invasion or non-invasion [15]. Most of the efforts have been focused on the development of flexible SERS substrates, including paper, glass fiber, and cellulose to fit various flexible, bent, or non-planar surfaces. For example, commercial tapes decorated with nanoparticles have been reported to enable the swabbing detection of pesticide residues and food contaminants in fruits and vegetables [16–19]. Ag nanoparticles self-assembled on cotton swabs have been used for the direct detection of trace explosives with 27 successive fingerprints [20]. In most cases, noble-metal nanoparticles have been reported to be decorated on surfaces of flexible substrates. However, in the absence of a protective layer, nanoparticles are easily damaged due to surface swabbing; hence, subsequent reuse is not possible.

Polydimethylsiloxane (PDMS) elastomer also has attracted immense interest for flexible SERS sensor applications due to its chemical stability, non-toxicity, mechanical flexibility, bendability, and hydrophobicity [21,22]. Especially, the hydrophobic property of PDMS not only can prevent the random spreading of an analyte solution to completely concentrate it, but also can permit recycling and reuse by washing with alcohol and water. Typically, versatile SERS detection involves the loading of plasmonic metal nanoparticles on the PDMS surface, affording localized surface plasmon resonance and subsequent electromagnetic field enhancement [23–26]. Fortuni et al. have reported the in situ synthesis of Au-shell Ag nanoparticles on a PDMS film with high SERS activity [26]. They found that Ag nanostructures modified on the surface of PDMS via vacuum filtration [27] and two steps of seed-mediated growth and magnetron sputtering [28] exhibited good adhesion and mechanical stretch ability. However, the "sticky" nature of PDMS alone is not enough to prevent the modified metal nanoparticles from being damaged or peeled off, especially against strong destruction of ultrasonication, corrosion by HNO_3, and surface swabbing. Thus, it is necessary to fabricate much stable special structures in which Ag nanostructures are embedded in the PDMS matrix.

Kumar et al. [29] fabricated an embedding structure by pouring liquid PDMS into silver nanorods on Si wafer and then peeling off after being cured. The embedding structure was not perfect with a small part of Ag nanorods exposed outside the PDMS film. Nonetheless, the film still held good mechanical stability and was used for the detection of trace pesticides from fruit peels via simple "paste and peel off" method. Motivated by the embedding structure, we focused our work on a better embedding structure with higher durability and recyclability and promoted its practicability in multiple cases. In this study, a cost-effective, simple, and rapid approach to prepare flexible, durable, and recyclable SERS substrates coupled with Ag nanowires (Ag NWs) and PDMS was proposed. Such an embedding structure can integrate the stretchability, durability, and hydrophobicity of PDMS and the high SERS activity of Ag NWs. As expected, the Ag NWs@PDMS film exhibited a good basic SERS performance including high SERS activity, good uniformity, stability, and recyclability, as well as unique durable properties such as anti-stretchability, anti-destruction by ultrasonication, anti-corrosion of HNO_3, and a broad working temperature range for MG sensing. The sensitive detection of trace MG in fruit juice by the standard addition method, with satisfactory recoveries, was possible. Notably, the flexible and durable SERS substrate was directly used to detect MG residues from fruits (i.e., apple and pear) by on-site surface swabbing with a reuse for five cycles. Moreover, the application of the Ag NWs@PDMS film was extended to the portable SERS detection of MG residues in successive 10 fingerprints on the basis of a flexible substrate combined with a portable Raman spectrometer.

2. Experimental section

2.1. Materials and reagents

Silver nanowires suspension (CST-NW-S30) in isopropanol was purchased from Suzhou ColdStones Technology Co., Ltd. Malachite green (MG) powder was obtained from Shanghai yuanye Bio-Technology Co., Ltd. Crystal violet (CV), methylene blue (MB) and carmine powders were purchased from Shanghai Aladdin Reagent Co., Ltd. Their molecular structures can be seen in Fig. S1. PDMS prepolymer (Sylgard 184 A) and cross-linker (Sylgard 184 B) were purchased form Dow Corning Corporation. Fruits (pear and apple) were purchased from local markets (Lanzhou, China). All chemicals were used without further purification. Water used in all experiments was purified on a Millipore Q system (18.2 MΩ cm).

2.2. Fabrication of Ag NWs@PDMS films

Scheme 1 shows the fabrication of Ag NWs@PDMS films. First, a glass slide was washed with acetone, ethanol, and water in that order. Second, 2 mL of the Ag NW suspension (5 mg/mL in isopropanol) was drop-coated and uniformly dispersed on a clean glass slide (75 mm × 25 mm), followed by drying in air at room temperature for 60 min. Third, 1 mL of the mixture with PDMS and the curing agent (ratio of PDMS: curing agent = 10:1 w/w) was dropped and spread out on the Ag NW surface. Finally, after it was dried, the embedding film (Ag NWs@PDMS) was peeled off from the glass slide and cut into some small pieces. To optimize the amount of Ag NWs, the volume of the Ag NW suspension was only changed. The cost of the Ag NWs@PDMS film (1 cm^2) was limited to 1 yuan/RMB on the basis of commercial costs of all materials. Completing a piece Ag NWs@PDMS film (75 mm × 25 mm) needed less than 1 min except the curing time of PDMS.

For comparison, an adhesive film (Ag NWs/PDMS) also was fabricated: First, the PDMS film was spread out on a glass slide, and then the Ag NWs suspension was drop-coated on the PDMS film. After being dried, the Ag NWs/PDMS film was peeled off from the glass slide.

2.3. Characterization

The microscopic features of the materials were characterized on a field emission scanning electron microscope (FE-SEM, JSM-6701F, JEOL Inc., Japan). X-ray photoelectron spectroscopy (XPS) was conducted for element analysis using a multifunctional spectrometer (Thermo Scientific) with Al Kα radiation source. X-ray diffractometry (XRD) was carried out on a Rigaku D/max-2400 using Cu K-α radiation source ($\lambda = 0.1541$ nm). Contact angle (CA) was measured with an optical contact angle meter at ambient temperature, where 3 μL water was

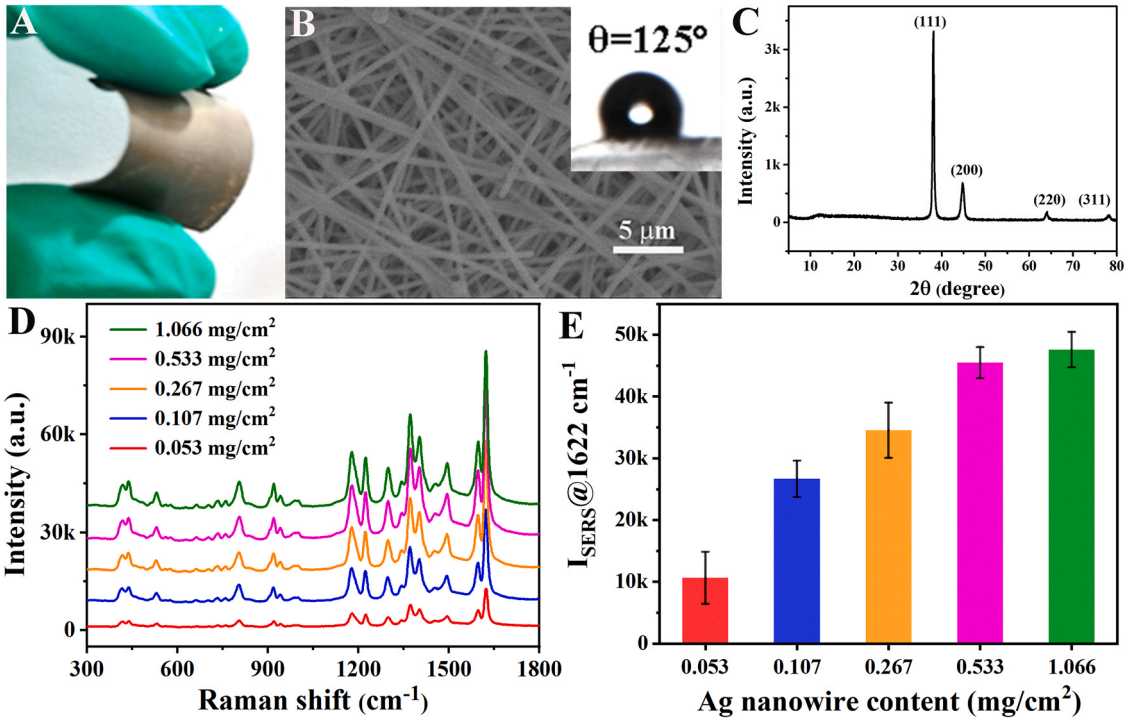


Fig. 1. Photograph (A), SEM image (B), and XRD pattern (C) of the Ag NWs@PDMS film. (D) SERS spectra of the film containing different contents of Ag adsorbed with 0.1 mM MG, and (E) corresponding peak intensities at 1622 cm^{-1}. Inset of (B) shows the shape of a water droplet with a CA of 125°. Error bars indicate standard deviations for six measurements.

dropped carefully onto the surface of the samples for calculating the CA with a contact angle plugin. The spectral transmittance of PDMS films was recorded on a UV-2102C model spectrometer at room temperature.

The Raman spectra were measured at room temperature on a Raman system (Zolix Finder Vista-HiR) under the laser of 532 nm with the laser power of 0.4 mW and a 100 × (NA = 0.90) objective lens. The typical acquisition time for MG measurements was 1 s with one accumulation. An Optosky self-developed portable Raman spectrometer (ATR3110, Optosky (Xiamen) Photonics Inc) was used for portable applications: Excitation wavelength of 785 nm and laser power of 10 mW. The acquisition time was 5 s with one accumulation.

2.4. SERS detection

For MG detection, the as-prepared Ag NWs@PDMS films were dipped in an aqueous MG solution with different concentrations (10^{-3} to 10^{-8} M), and SERS measurements were conducted after the films were dried. To examine the effect of interference, a series of inorganic and organic species (0.1 mM) were separately added into the aqueous MG solution (0.1 mM). Analogous dyes (such as CV, MB, and carmine) with equal concentrations (10 μM) were spiked in the 10 μM MG solution. The films were immersed into the solution spiked with interfering species for SERS measurements under the same conditions.

For point-to-point uniformity, 20 positions on the same film with 0.1 mM MG were randomly selected for SERS measurements. For batch-to-batch uniformity, five batches of Ag NWs@PDMS films were prepared.

For the anti-stretchability test, the film adsorbed with 0.1 mM MG was stretched to 30% of its length for recording Raman spectra. For the anti-destruction test, Ag NWs@PDMS films were subjected to ultrasonication under a power output of 200 W at different times. After the films were washed with water, the films were adsorbed with 0.1 mM MG for SERS measurement. For the anti-corrosion test, Ag NWs@PDMS films were soaked in an HNO_3 solution at different pHs (1–6) for 1 h. After the films were washed with water and dried, the films were adsorbed with 0.1 mM MG for SERS measurement. To investigate the effect of the working temperature, the Ag NWs@PDMS film adsorbed with 0.1 mM MG was subjected to different temperatures (−20 to 80 °C) for 1 h prior to the measurement.

For the recyclability test, the Ag NWs@PDMS film was measured in 10 successive cycles. The film was adsorbed with 1 mM MG and subjected to SERS measurement. The recycled film was washed five times with ethanol and water, and reused for the next cycle. For the stability test, the Ag NWs@PDMS film adsorbed with 0.1 mM MG was used for SERS measurement every 3 days for 1 month under the same conditions, where the film was maintained under ambient conditions.

For the detection of MG in juice, after squeezing the juice from apple and pear, the juices were statically settled overnight at room temperature. Then, the supernatant was filtered through a 0.22-μm membrane, followed by diluting 10 times with water. A defined MG amount was added to the above juice to further calculate the recovery.

For surface swabbing experiments, a 20 μL MG solution with a certain concentration was dropped on the fruits surface (0.5 × 0.5 cm^2). The MG residue remained on the surface after the evaporation of the aqueous solution. Then, a blank Ag NWs@PDMS film was soaked with ethanol (10 μL) and used to swab the fruits surface to collect the MG residue. SERS spectra of the swabbed substrate on five spots were randomly collected.

For portable detection, a 3D printed holder was installed in the Raman probe of the portable apparatus to fix the detection film. Its aim was to find and then fix the optimum focusing position. A MG drop (20 μL, 10^{-2} M) was dropped on a finger, and then it was successively touched on 10 films for detection under the same conditions.

3. Results and discussion

3.1. Characterization and optimized SERS performance of Ag NWs@PDMS

Owing to the excellent flexibility of PDMS, the Ag NWs@PDMS film

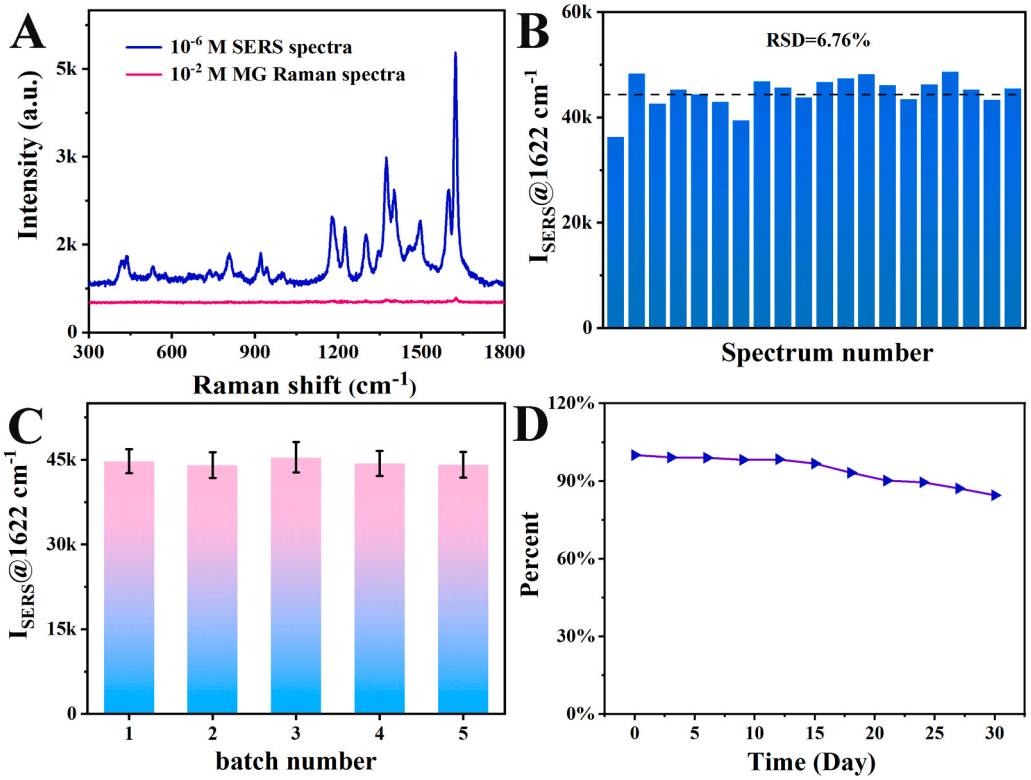


Fig. 2. (A) SERS spectrum of 10^{-6} M MG adsorbed on Ag NWs@PDMS and Raman spectrum of an aqueous 10^{-2} M MG solution. (B) Point-to-point and (C) batch-to-batch uniformity. (D) SERS stability during a 1-month period. Error bars indicate the standard deviation for six measurements.

is still flexible as can be observed from its photograph (Fig. 1A). The Ag NWs@PDMS film was further examined by SEM, XRD, and XPS. From the SEM image (Fig. 1B), the diameter and length of the Ag NWs are ~30 nm and 20–30 μm, respectively. The Ag NWs are interconnected with each other to form a network. The water contact angle (CA) of the Ag NWs@PDMS film is 125° (the inset of Fig. 1B), which is equal to that of the pure PDMS film (124°, Fig. S2A). In contrast, when Ag NWs are only assembled on the PDMS surface, the Ag NWs also are randomly distributed on the PDMS film with the CA of only 70° (Fig. S2B). This proves that the Ag NWs are located outside due to the hydrophilicity of Ag NWs [30]. From the cross-sectional SEM images (Fig. S3), the vast majority of Ag NWs are wrapped and the surface is smooth for Ag NWs@PDMS; the layer of Ag NWs can be clear observed for unwrapped Ag NWs/PDMS.

The XRD pattern (Fig. 1C) of Ag NWs reveals characteristic diffraction peaks at 2θ of 38.2°, 44.5°, 64.5°, and 77.5°, corresponding to the (111), (200), (220), and (311) planes of Ag face-centered cubic (*fcc*) crystalline phases (JCPDS 04-0783). The XPS Ag 3d spectrum (Fig. S4) confirms the formation of metallic silver, where the peaks at 368.12 eV and 374.13 eV correspond to the binding energies of Ag $3d_{5/2}$ and Ag $3d_{3/2}$ of Ag (0), respectively [31].

Fig. S5 shows the typical SEM images of Ag NWs@PDMS films with different densities of Ag NWs in the range from 0.053 to 1.066 mg/cm^2. With the increase in the distribution density, a high number of Ag NWs junctions are formed. The SERS activity of Ag NWs@PDMS films was investigated by the variation in the Ag NWs density. Fig. 1D shows the SERS spectra of the films with different contents of Ag. The characteristic peaks of MG are distinguishable, and peaks corresponding to Ag NWs@PDMS without MG are not observed (Fig. S6). The peak at 917 cm^{-1} corresponds to the ring skeletal radial vibrations. Peaks at 1175 cm^{-1} and 1294 cm^{-1} correspond to the ring C–H stretching vibrations. Peaks corresponding to the N–C stretching and C–C/C–H stretching vibrations are observed at 1369 cm^{-1} and 1400 cm^{-1}, respectively. The peak at 1617 cm^{-1} corresponds to N–C and C–C bond stretching vibrations [32]. Fig. 1E shows the plot of the SERS signal intensity at 1622 cm^{-1} against the Ag NWs density. As expected, with the increase in the Ag NW density, the SERS signal intensity increases. But, the overloading of Ag NWs (density of 1.066 mg/cm^2) does not further improve the signal intensity. Accordingly, a Ag NW density of 0.533 mg/cm^2 was selected for subsequent experiments.

Furthermore, the signal intensity between Ag NWs@PDMS and unwrapped Ag NWs/PDMS was compared. It is known that the SERS activity of the Ag NWs@PDMS stems from Ag NWs rather than PDMS. Generally, the SERS activity of the wrapped structure should be decreased compared to the unwrapped structure. However, it is found that the SERS activity of Ag NWs@PDMS almost kept unchanged as compared with unwrapped Ag NWs/PDMS for the MG concentration of 10^{-4} M or 10^{-7} M (Fig. S7). Distinctly, the hydrophobic force is important for SERS detection, in which the substrate hydrophobicity could concentrate analytes to enhance the SERS signal [33–36]. Another factor may be the transparent PDMS with high optical transmittance [21]. A pure PDMS film with a thickness of 0.15 mm exhibits 99.7% transparency in the visible-light region (400–750 nm, Fig. S8).

3.2. *Basic SERS performance: sensitivity, uniformity, stability, and recyclability*

Basic SERS performance of Ag NWs@PDMS, including the sensitivity, uniformity, and stability, was systematically investigated by using MG as the probe molecule. The enhancement factor (*EF*) is a key indicator to evaluate the SERS sensitivity [33]. Fig. 2 A shows the SERS spectrum of 10^{-6} M MG adsorbed on Ag NWs@PDMS as well as the Raman spectrum of a 10^{-2} M aqueous MG solution. Using the 1622 cm^{-1} peak as the reference, the EF value was calculated to be 4.77×10^5. The detailed calculation has been added in the Supporting Information.

The point-to-point uniformity of a substrate was examined by randomly selecting 20 positions. As shown in Fig. S9A, the peak

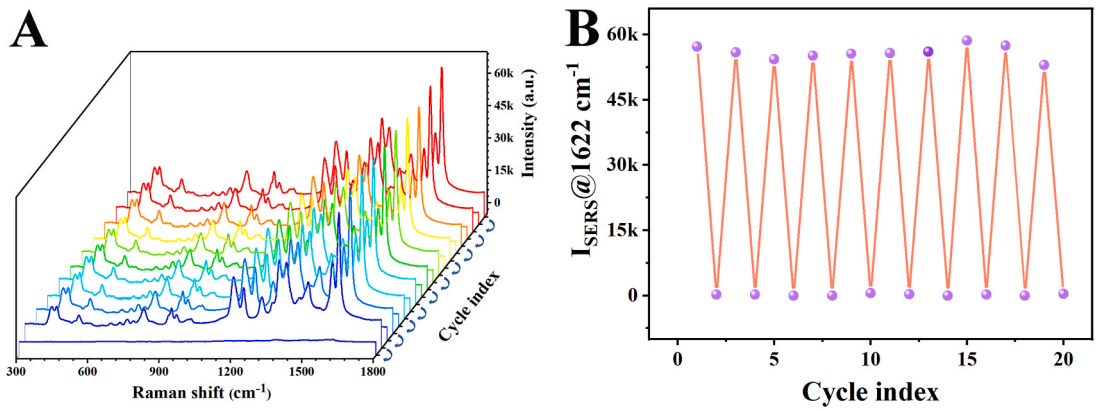


Fig. 3. (A) SERS spectra of MG (1 mM) on Ag NWs@PDMS before and after cleaning with ethanol and water for 10 cycles. (B) Recycling performance for MG sensing.

intensities at 1622 cm^{-1} are almost unchanged with a relative standard deviation (RSD) of only 6.76% (Fig. 2B). According to the Raman mapping for accessing the uniformity (Fig. S10A), the RSD value is calculated to be 10.04% from the corresponding histogram @1622 cm^{-1} (Fig. S10B). For unwrapped Ag NWs/PDMS, an RSD value of up to 12.67% is obtained for point-to-point uniformity (Figs. S11A and S11B). To examine the batch-to-batch uniformity, five Ag NWs@PDMS substrates from different production batches were determined, which were adsorbed with 0.1 mM MG. And their corresponding SERS spectra are in Fig. S9B. The RSD value is still limited to 5.0% from the peak intensity at 1622 cm^{-1} (Fig. 2 C). This result suggests that the simple preparation method of the embedding Ag NWs@PDMS substrate is reliable to achieve good point-to-point as well as batch-to-batch uniformity.

Air oxidation of Ag in Ag-based SERS substrates is one of the greatest challenges [14]. Fig. S9C shows the SERS spectra of Ag NWs@PDMS adsorbed with 0.1 mM MG, which are kept in an ambient environment and measured every three days at room temperature. During the measurement period, the SERS intensity slowly decreases (Fig. 2D). Even after 30 days, the peak intensity at 1622 cm^{-1} is still maintained at 85% of its initial intensity. By comparison, the intensity after 30 days decreases to 40% for unwrapped Ag NWs/PDMS (Figs. S11C and S11D), indicating that the Ag NWs@PDMS substrate exhibits excellent SERS stability. Photobleaching of dyes such as R6G and MG is a negative effect leading to SERS instability [1,37]. Ag nanostructures can generate hotspots to achieve good SERS effect; meanwhile the hotspots intensify the photobleaching effect of dye molecules. Mao et al. reported that the silicone polymer matrix was a good sensory support for preventing photobleaching of the probes [38]. Therefore, the excellent SERS stability can be ascribed to the presence of the PDMS matrix, which reduces the probability of photobleaching of MG molecules and thus improves the SERS photostability.

Recyclability is another crucial factor for label-free SERS applications [39]. The embedding structure permits the multiple recycling of Ag NWs@PDMS. The cleaning of adsorbed MG from the substrate can be easily achieved by washing with ethanol and water due to the hydrophobicity of PDMS. Fig. 3A shows the SERS spectra of Ag NWs@PDMS

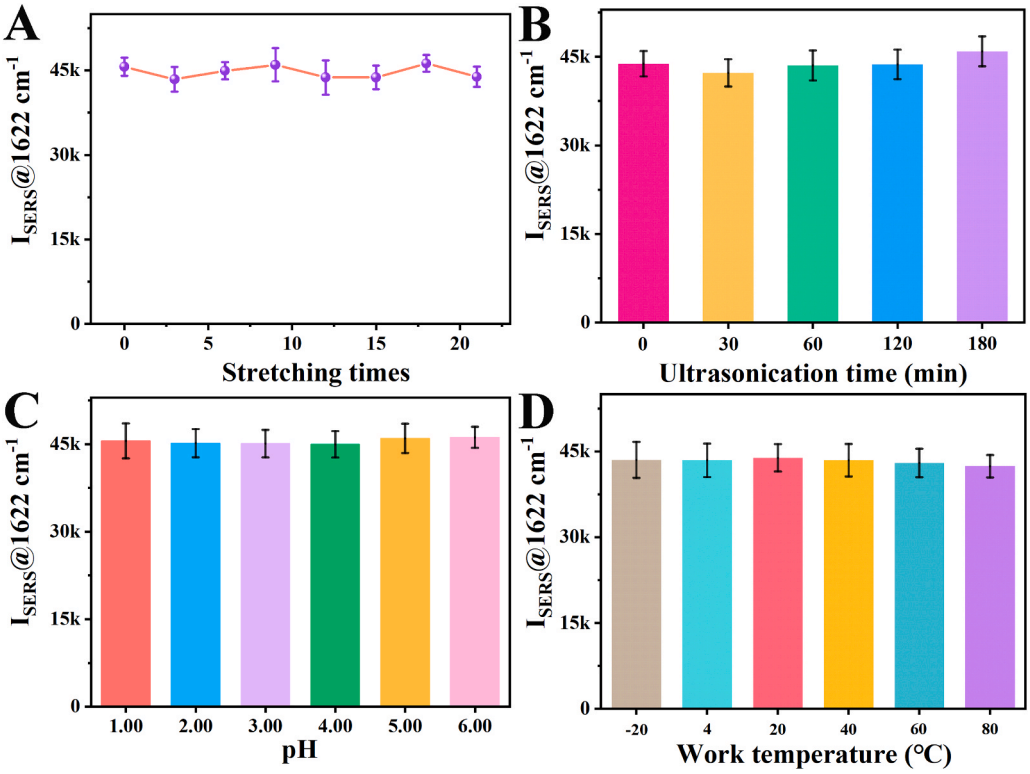


Fig. 4. Effects of stretching times (A), ultrasonication time (B), pH of HNO_3 solution (C), and working temperature (D) on the peak intensity at 1622 cm^{-1}.

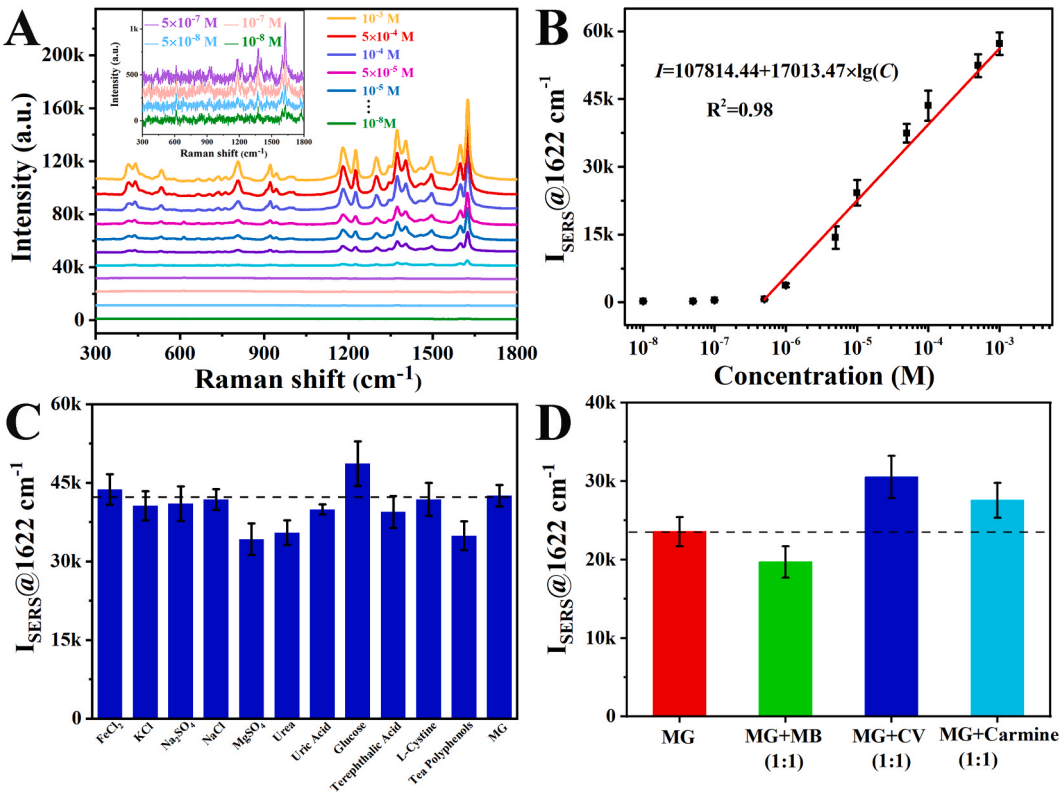


Fig. 5. (A) SERS spectra of MG with different concentrations on Ag NWs@PDMS. (B) Plot of peak intensities against the MG concentration. (C) SERS intensities of MG in the presence of interfering reagents, with each of their concentrations being 0.1 mM. (D) SERS intensities of MG in the presence of CV, MB, and carmine, with each of their concentrations being 10 μM. All error bars indicate the standard deviation for six measurements.

by the adsorption of MG and cleaning with ethanol and water. Strong SERS signals are observed after the adsorption of MG, while peaks characteristic of MG are distinguished after washing with ethanol. According to the variation in the peak intensity at 1622 cm^{-1} through ten cycles (Fig. 3B), the observed peak intensity is still essentially unchanged after ten cycles in comparison to the initial cycle. The results indicate that the Ag NWs@PDMS film is practical as a recyclable SERS substrate.

3.3. Unique properties: anti-stretchability, anti-destruction, anti-corrosion, and a broad working temperature range

PDMS is one of the most widely used silicon-based organic polymers. It is particularly known for its unique properties such as flexibility, toughness, tensile elasticity, and thermal stability [22]. Here, the effect of stretchability on the SERS activity was examined by stretching the Ag NWs@PDMS film. Fig. S12A shows the resulting SERS spectra. After 21 times of successive stretching without morphological change (Fig. S13A), the peak intensity at 1622 cm^{-1} exhibits near steadiness (Fig. 4A). Ultrasonication is extremely destructive, which can peel off the loaded nanoparticles from their support. However, the Ag NWs@PDMS film still maintains a high SERS intensity even after ultrasonication at 200 W for 180 min (Figs. 4B and S12B). This result can be attributed to the embedding structure, which prevents the Ag NWs from being peeled off from the support (Figs. S13B and S14). Inductively coupled plasma atomic emission spectroscopy (ICP-AES) was used to determine the detailed Ag amount from being peeled off via ultrasonication. The loss of Ag was only 0.35 wt% for Ag NWs@PDMS under 180 min ultrasonication. When the unwrapped Ag NWs/PDMS film was subjected to ultrasonication for only 60 min, most Ag NWs were peeled off (Fig. S14) with the loss of 84 wt%. The ICP-AES analysis process can be seen in the Supporting Information.

Similarly, the film also exhibits good anti-corrosion against HNO_3. After immersing the film into HNO_3 at different pH values for 1 h, the SERS intensity at 1622 cm^{-1} still maintains high values (Figs. 4C and S12C). Evidently, good anti-stretchability, anti-destruction, and anti-corrosion of the Ag NWs@PDMS film can be mainly attributed to the wrapping of PDMS as a protective layer. In addition, the effect of the working temperature on the SERS activity was investigated. When the Ag NWs@PDMS substrates are kept at temperatures in the range of −20–80 °C for 1 h, the SERS intensity exhibits a slight variation (Figs. 4D and S12D). All these results suggest that the film is suitable for SERS detection under less favorable conditions (vibratile and tensile environment, extreme temperatures and pHs).

3.4. SERS applications

3.4.1. Quantitative detection of MG

Based on the above properties of the Ag NWs@PDMS film, MG was selected as the model analyte to investigate SERS applications of the film. A series of aqueous MG solutions from 10^{-3} to 10^{-8} M were detected on the basis of the Ag NWs@PDMS film (Fig. 5A). A linear curve is obtained for the plot of the peak intensity at 1622 cm^{-1} (I) against the logarithm of the MG concentration (lg (c)) in the range from 0.5 to 1000 μM (Fig. 5B). The linear equation can be described as follows: $I = 107{,}814.44 + 17{,}013.47 \times \lg(c)$ ($R^2 = 0.98$). The limit of detection (LOD) reaches up to 10 nM based on S/N = 3, which is superior to, or compatible with, those obtained for conventional methods such as capillary electrophoresis, fluorescence spectroscopy, and SERS for MG sensing (Table S1).

In addition, the SERS specificity was discussed. Various inorganic and organic interfering species (0.1 mM for each) were added into a 0.1 mM MG solution. Comparison of the characteristic peak intensities at 1622 cm^{-1} before and after the addition of these interfering species

Table 1
Determination of MG in apple and pear juice based on Ag NWs@PDMS.

Analyte	Original (μM)	Spiked (μM)	Found (μM)	Recovery (%)	RSD (%)
Pear juice	No Found	100.00	95.00	95.00	6.73
		0.50	0.51	102.00	8.02
Apple juice	No Found	100.00	105.78	105.78	9.46
		0.50	0.49	98.00	8.41

(Figs. 5C and S15) reveals controlled in fluctuations of 15%. Considering the coexistence of other dyes, three dyes (viz. CV, MB, and carmine, respectively) with equal concentrations (10 μM) were added in the control solution (only MG). No significant shifts of the peak at 1622 cm^{-1} are observed owing to the fingerprint characteristics of MG molecules (Fig. 5D).

The feasibility of the quantitative MG detection in fruit (i.e., apple and pear) juice was investigated by the standard addition method. Fig. S16 shows the corresponding SERS spectra of the juice spiked with MG. Table 1 lists the obtained results: Satisfactory recoveries from 95.00% to 105.78% are obtained, in addition to low RSD values of less than 10%.

The SERS platform based on Ag NWs@PDMS can be also used for the detection of other dyes like CV, MB and rhodamine 6G (R6G). Even for a low concentration, good band resolution and a high Raman signal could be clearly obtained (Fig. S17).

3.4.2. *Quantitative detection of MG on the fruit surface via surface swabbing*

Owing to the presence of the PDMS coating, directly scratching the fruit (apple and pear) surfaces using the Ag NWs@PDMS films does not lead to any damage to the Ag NWs, permitting a rapid and a point-of-care detection of the dye residue on fruits. Herein, surfaces (0.5 × 0.5 cm^2) of fruits such as apple and pear were spiked with different MG residues (from 3 ng/cm^2 to 30 μg/cm^2), and then Ag NWs@PDMS films were used to scratch the surfaces to collect the MG residue. Fig. 6A and D show the corresponding SERS spectra. With the increase in the MG concentration, the SERS intensity at 1622 cm^{-1} increases. Even after spiking the solution with only 3 ng/cm^2 of MG, the SERS signals still can be identified. Using 1622 cm^{-1} for the calibration, a good linear relationship between the intensity and the logarithm of the MG residue amount is achieved (Fig. 6B and E). Table 2 lists the corresponding data obtained from quantitative analysis. Similar values for both series of parameters are obtained from the swabbing detection on apple and pear, indicative of the feasibility and reliability of the quantitative detection of MG residue on fruits. Notably, the Ag NWs@PDMS films can be reused by washing with ethanol and water. According to their SERS spectra after five cycles (Figs. S18A and S18B), the SERS intensity at 1622 cm^{-1} marginally changes (Figs. 6C and F).

3.4.3. *Portable SERS detection in fingerprints*

SERS detection using a portable Raman spectrometer is gradually favored and available [40,41]. Aromatic dyes such as MG and R6G are used as developing agents to enhance the visualization of fingerprints. Hence, the portable SERS detection of MG residues in fingerprints demonstrates promise and practical utility for fingerprint identification in forensic investigation.

In this study, in terms of the above-mentioned excellent properties of the Ag NWs@PDMS film, its potential application combined with a portable Raman spectrometer was explored for the portable detection of the MG residue. Fig. 7A shows the photograph of the portable detection apparatus to fix the film using a 3D printed holder. The optimum focusing position can be found and fixed, which is crucial for portable

Table 2
Quantitation analysis results of MG residue on the fruits through surface swabbing.

	Apple	Pear
Linear equation	I= 1120.78 + 1333.51 × lg (C)	I= 1047.80 + 1220.51 × lg (C)
Linear range (μg/cm^2)	0.15–30	0.15–30
LOD (ng/cm^2)	3	15

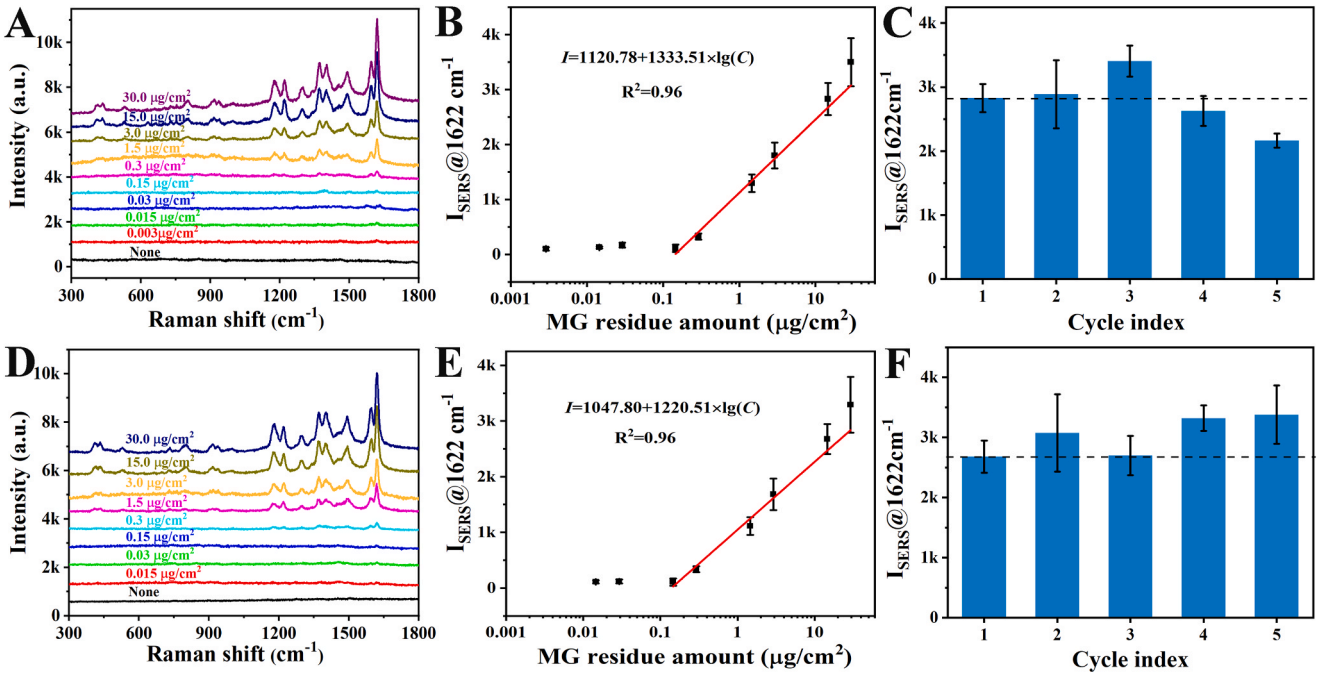


Fig. 6. SERS spectra of MG with different amounts of residue by surface swabbing from apple (A) and pear (D) surfaces. (B) and (E) show their relationship plots between the peak intensities and MG residue amount. Reusability of the film for the surface swabbing on apple (C) and pear (F) in five successive cycles. Error bars indicate the standard deviation for six measurements.

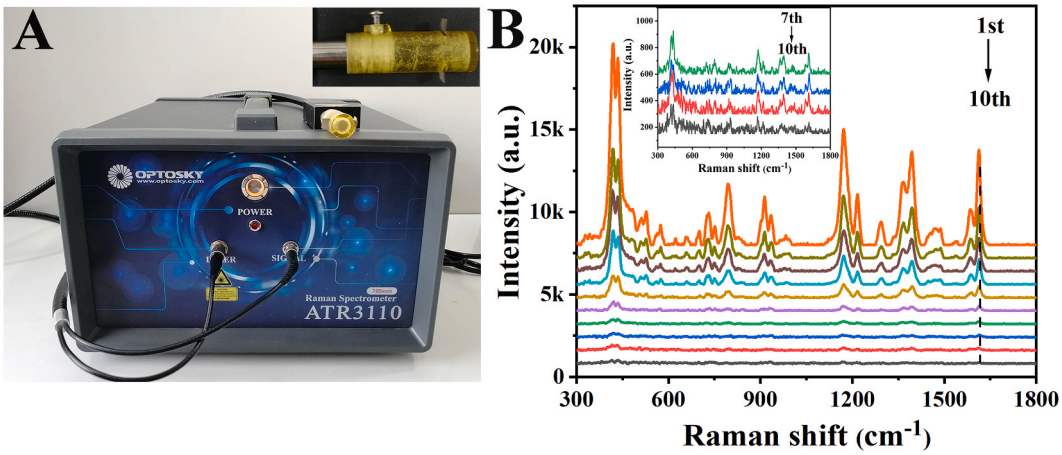


Fig. 7. (A) Photograph of the portable detection apparatus with a 3D printed holder to fix the flexible SERS film. (B) SERS spectra of MG obtained by swabbing the fingerprint on Ag NWs@PDMS. Integration time, 5 s; laser power, 10 mW; laser wavelength, 785 nm. Spectra were recorded from the 1st to10th by pressing a contaminated finger with a 10^{-2} M MG drop (20 μL).

SERS detection. By pressing the Ag NWs@PDMS film surface with a contaminated finger containing a drop of 10^{-2} M MG, portable detection was performed. Fig. 7B shows the SERS spectra from the 1st to 10th pressing. Clearly, well-resolved Raman signatures of MG are still clearly distinguished even for the 10th pressing, indicative of the good combination of the portable Raman spectrometer and excellent film properties.

4. Conclusions

A flexible, durable, and recyclable SERS substrate was designed by embedding Ag NWs into a PDMS film. SERS measurements reveal that the film exhibits not only excellent basic SERS performance such as high SERS activity, uniformity, long-term stability, and recyclability but also good application potential under less favorable conditions. In view of these advantages, the AgNWs@PDMS substrate successfully served as a multifunctional detection platform. One of the platform involved the detection of MG residue in juices, with a wide linear range of 0.5–1000 μM, a low LOD of 10 nM, and good selectivity. The other platform involved the swabbing detection of the MG residue on fruits by recycling. The third platform included portable SERS detection in fingerprints. This flexible, durable, recyclable, and on-site swabbing SERS detection platform is thought to demonstrate promise in food safety and forensic science, especially in portable SERS analytical applications with high efficiency.

CRediT authorship contribution statement

Juanjuan Luo: Conceptualization, Investigation, Visualization Writing – original draft. **Zekai Wang:** Investigation. **Yun Li:** Resources. **Changding Wang:** Visualization. **Jiefang Sun:** Writing – review & editing. **Weichun Ye**: Conceptualization, Writing – original draft, Writing – review & editing, Project administration, Supervision. **Xiaolong Wang:** Resources, Writing – review & editing. **Bing Shao:** Writing – review & editing.

Declaration of Competing Interest

The authors declare that they have no known competing financial interests or personal relationships that could have appeared to influence the work reported in this paper.

Acknowledgements

This work is supported by the Fundamental Research Funds for Central Universities (No. lzujbky-2020-it25) and Natural Science Foundation of Gansu Province, China (No. 20JR5RA622).

Appendix A. Supporting information

Supplementary data associated with this article can be found in the online version at doi:10.1016/j.snb.2021.130602.

References

[1] L. Ouyang, L. Yao, T. Zhou, L. Zhu, Accurate SERS detection of malachite green in aquatic products on basis of graphene wrapped flexible sensor, Anal. Chim. Acta 1027 (2018) 83–91.
[2] E. Sudova, J. Machova, Z. Svobodova, T. Vesely, Negative effects of malachite green and possibilities of its replacement in the treatment of fish eggs and fish: a review, Vet. Med. 52 (2007) 527–539.
[3] G.D. Vyavahare, R.G. Gurav, P.P. Jadhav, R.R. Patil, C.B. Aware, J.P. Jadhav, Response surface methodology optimization for sorption of malachite green dye on sugarcane bagasse biochar and evaluating the residual dye for phyto and cytogenotoxicity, Chemosphere 194 (2018) 306–315.
[4] J. Lin, C. Zhang, M. Xu, Y. Yuan, J. Yao, Surface-enhanced Raman spectroscopic identification in fingerprints based on adhesive Au nanofilm, RSC Adv. 8 (2018) 24477–24484.
[5] C. Byram, S.S.B. Moram, V.R. Soma, SERS based detection of multiple analytes from dye/explosive mixtures using picosecond laser fabricated gold nanoparticles and nanostructures, Analyst 144 (2019) 2327–2336.
[6] E. Mirparizi, M. Rajabi, M. Bazregar, A. Asghari, Centrifugeless ultrasound-assisted emulsification microextraction based on salting-out phenomenon followed by high-performance liquid chromatography for the simple determination of phthalate esters in aqueous samples, J. Sep. Sci. 40 (2017) 2022–2029.
[7] E. Dubreil, S. Mompelat, V. Kromer, Y. Guitton, M. Danion, T. Morin, D. Hurtaud-Pessel, E. Verdon, Dye residues in aquaculture products: targeted and metabolomics mass spectrometric approaches to track their abuse, Food Chem. 294 (2019) 355–367.
[8] F. Wang, H. Wang, Y.D. Shen, Y.J. Li, J.X. Dong, Z.L. Xu, J.Y. Yang, Y.M. Sun, Z. L. Xiao, Bispecific monoclonal antibody-based multianalyte ELISA for furaltadone metabolite, malachite green, and leucomalachite green in aquatic products, J. Agric. Food Chem. 64 (2016) 8054–8061.
[9] Y. Hu, Z. Gao, J. Luo, Fluorescence detection of malachite green in fish tissue using red emissive Se,N,Cl-doped carbon dots, Food Chem. 335 (2021), 127677.
[10] D. Zhang, H. You, L. Yuan, R. Hao, T. Li, J. Fang, Hydrophobic slippery surface-based surface-enhanced Raman spectroscopy platform for ultrasensitive detection in food safety applications, Anal. Chem. 91 (2019) 4687–4695.
[11] C. Zong, M. Xu, L.J. Xu, T. Wei, X. Ma, X.S. Zheng, R. Hu, B. Ren, Surface-enhanced Raman spectroscopy for bioanalysis: reliability and challenges, Chem. Rev. 118 (2018) 4946–4980.
[12] J. Neng, Q. Zhang, P. Sun, Application of surface-enhanced Raman spectroscopy in fast detection of toxic and harmful substances in food, Biosens. Bioelectron. 167 (2020), 112480.
[13] Y. Jiang, D.-W. Sun, H. Pu, Q. Wei, Surface enhanced Raman spectroscopy (SERS): a novel reliable technique for rapid detection of common harmful chemical residues, Trends Food Sci. Technol. 75 (2018) 10–22.
[14] C. Liu, X. Xu, W. Hu, X. Yang, P. Zhou, G. Qiu, W. Ye, Y. Li, C. Jiang, Synthesis of clean cabbagelike (111) faceted silver crystals for efficient surface-enhanced Raman scattering sensing of papaverine, Anal. Chem. 90 (2018) 9805–9812.

[15] Y. Wang, X. Yu, Y. Chang, C. Gao, J. Chen, X. Zhang, J. Zhan, A 3D spongy flexible nanosheet array for on-site recyclable swabbing extraction and subsequent SERS analysis of thiram, Mikrochim. Acta 186 (2019) 458.
[16] J. Chen, Y. Huang, P. Kannan, L. Zhang, Z. Lin, J. Zhang, T. Chen, L. Guo, Flexible and adhesive surface enhance Raman scattering active tape for rapid detection of pesticide residues in fruits and vegetables, Anal. Chem. 88 (2016) 2149–2155.
[17] X. Gong, M. Tang, Z. Gong, Z. Qiu, D. Wang, M. Fan, Screening pesticide residues on fruit peels using portable Raman spectrometer combined with adhesive tape sampling, Food Chem. 295 (2019) 254–258.
[18] J. Jiang, S. Zou, Y. Li, F. Zhao, J. Chen, S. Wang, H. Wu, J. Xu, M. Chu, J. Liao, Z. Zhang, Flexible and adhesive tape decorated with silver nanorods for in-situ analysis of pesticides residues and colorants, Microchim. Acta 186 (2019) 603.
[19] X. He, S. Yang, T. Xu, Y. Song, X. Zhang, Microdroplet-captured tapes for rapid sampling and SERS detection of food contaminants, Biosens. Bioelectron. 152 (2020), 112013.
[20] Z. Gong, H. Du, F. Cheng, C. Wang, C. Wang, M. Fan, Fabrication of SERS swab for direct detection of trace explosives in fingerprints, ACS Appl. Mater. Interfaces 6 (2014) 21931–21937.
[21] D. Han, Y. Li, X. Jiang, W. Zhao, F. Wang, W. Lan, E. Xie, W. Han, A facile method to prepare transparent and stretchable epidermal thin film heaters, Compos. Sci. Technol. 168 (2018) 460–466.
[22] S. Zhang, C. Lin, Z. Xia, M. Chen, Y. Jia, B. Tao, S. Li, K. Cai, A facile and novel design of multifunctional electronic skin based on polydimethylsiloxane with micropillars for signal monitoring, J. Mater. Chem. B 8 (2020) 8315–8322.
[23] J. Sun, L. Gong, Y. Lu, D. Wang, Z. Gong, M. Fan, Dual functional PDMS sponge SERS substrate for the on-site detection of pesticides both on fruit surfaces and in juice, Analyst 143 (2018) 2689–2695.
[24] S. Lin, W. Hasi, S. Han, X. Lin, L. Wang, A dual-functional PDMS-assisted paper-based SERS platform for the reliable detection of thiram residue both on fruit surfaces and in juice, Anal. Methods 12 (2020) 2571–2579.
[25] N. Duan, M. Shen, S. Qi, W. Wang, S. Wu, Z. Wang, A. SERS, A SERS aptasensor for simultaneous multiple pathogens detection using gold decorated PDMS substrate, Spectrochim. Acta A Mol. Biomol. Spectrosc. 230 (2020), 118103.
[26] B. Fortuni, T. Inose, S. Uezono, S. Toyouchi, K. Umemoto, S. Sekine, Y. Fujita, M. Ricci, G. Lu, A. Masuhara, J.A. Hutchison, L. Latterini, H. Uji-I, In situ synthesis of Au-shelled Ag nanoparticles on PDMS for flexible, long-life, and broad spectrum-sensitive SERS substrates, Chem. Commun. 53 (2017) 11298–11301.
[27] R.R. Kisannagar, P. Jha, A. Navalkar, S.K. Maji, D. Gupta, Fabrication of silver nanowire/polydimethylsiloxane dry electrodes by a vacuum filtration method for electrophysiological signal monitoring, ACS Omega 5 (2020) 10260–10265.
[28] Y. Ma, Y. Du, Y. chen, C. Gu, T. Jiang, G. Wei, J. Zhou, Intrinsic Raman signal of polymer matrix induced quantitative multiphase SERS analysis based on stretched PDMS film with anchored Ag nanoparticles/Au nanowires, Chem. Eng. J. 381 (2020), 122710.
[29] S. Kumar, P. Goel, J.P. Singh, Flexible and robust SERS active substrates for conformal rapid detection of pesticide residues from fruits, Sens. Actuator B Chem. 241 (2017) 577–583.
[30] E. Mahmoudi, L.Y. Ng, W.L. Ang, Y.H. Teow, A.W. Mohammad, Improving membrane bioreactor performance through the synergistic effect of silver-decorated graphene oxide in composite membranes, J. Water Process Eng. 34 (2020), 101169.
[31] C. Liu, X. Xu, C. Wang, G. Qiu, W. Ye, Y. Li, D. Wang, ZnO/Ag nanorods as a prominent SERS substrate contributed by synergistic charge transfer effect for simultaneous detection of oral antidiabetic drugs pioglitazone and phenformin, Sens. Actuators B Chem. 307 (2020), 127634.
[32] Y. Zhang, W. Yu, L. Pei, K. Lai, B.A. Rasco, Y. Huang, Rapid analysis of malachite green and leucomalachite green in fish muscles with surface-enhanced resonance Raman scattering, Food Chem. 169 (2015) 80–84.
[33] X. Jiang, Y. Lai, W. Wang, W. Jiang, J. Zhan, Surface-enhanced Raman spectroscopy detection of polybrominated diphenylethers using a portable Raman spectrometer, Talanta 116 (2013) 14–17.
[34] L. Xiao, M. Zhang, Z. Liu, W. Bian, X. Zhang, J. Zhan, Hydrophobic silver nanowire membrane for swabbing extraction and in situ SERS detection of polycyclic aromatic hydrocarbons on toys, Anal. Methods 9 (2017) 1816–1824.
[35] P. Kumar, R. Khosla, M. Soni, D. Deva, S.K. Sharma, A highly sensitive, flexible SERS sensor for malachite green detection based on Ag decorated microstructured PDMS substrate fabricated from Taro leaf as template, Sens. Actuator B Chem. 246 (2017) 477–486.
[36] L. Jing, Y. Shi, J. Cui, X. Zhang, J. Zhan, Hydrophobic gold nanostructures via electrochemical deposition for sensitive SERS detection of persistent toxic substances, RSC Adv. 5 (2015) 13443–13450.
[37] J. Li, W. Zhang, H. Lei, B. Li, Ag nanowire/nanoparticle-decorated MoS_2 monolayers for surface-enhanced Raman scattering applications, Nano Res. 11 (2018) 2181–2189.
[38] Y. Mao, Q. Zhao, T. Pan, J. Shi, S. Jiang, M. Chen, B. Zhou, Y. Tian, Platinum porphyrin/3-(trimethoxysily)propylmethacrylate functionalized flexible PDMS micropillar arrays as optical oxygen sensors, New J. Chem. 41 (2017) 5429–5435.
[39] Y. Du, H. Liu, Y. Chen, Y. Tian, X. Zhang, C. Gu, T. Jiang, J. Zhou, Recyclable label-free SERS-based immunoassay of PSA in human serum mediated by enhanced photocatalysis arising from Ag nanoparticles and external magnetic field, Appl. Surf. Sci. 528 (2020), 146953.
[40] Y. Wu, Y. Liu, X. Tang, Z. Cheng, H. Liu, Tunable plasmonics of hollow raspberry-like nanogold for the robust Raman scattering detection of antibiotics on a portable Raman spectrometer, Analyst 145 (2020) 5854–5860.
[41] Y. Shi, W. Wang, J. Zhan, A positively charged silver nanowire membrane for rapid on-site swabbing extraction and detection of trace inorganic explosives using a portable Raman spectrometer, Nano Res. 9 (2016) 2487–2497.

Juanjuan Luo is a postgraduate student of Lanzhou University. Her research majors in SERS analysis application.

Zeikai Wang is a undergraduate student of College of chemistry&chemical engineering, Lanzhou University.

Yun Li received his Master degree from Lanzhou University, China in 2011. He is currently a Senior Engineer at Lanzhou Institutes for Food and Drug Control, China. His research interests focus on drug analysis and quality control.

Changding Wang is a postgraduate student of Lanzhou University currently, majoring in SERS analysis and materials chemistry.

Jiefang Sun received her Doctor degree of analytical chemistry from Beijing Institute of Pharmacology and Toxicology, China in 2011. She is currently an associate professor at Beijing Center for Disease Control & Prevention, China. Her research field is focusing on micro-/nano-scale materials based sensing.

Weichun Ye is an associate professor in Department of Chemistry, Lanzhou University. He received his Ph.D. degree from Lanzhou University in 2008. After a two-year postdoctoral research in Lanzhou Institute of Chemical Physics, Chinese Academy of Sciences, he joined the faculty of Department of Chemistry at Lanzhou University in 2010. His research interests include chemical sensor, electroanalysis and surface-enhanced Raman scattering.

Xiaolong Wang received his Ph.D. degree from Lanzhou University, China in 2007. At present, he is a researcher at Lanzhou Institute of Chemical Physics, Chinese Academy of Sciences, China. His research fields include material chemistry, surface engineering, flexible electronics and 3D printing.

Bing Shao received his Doctor degree of analytical chemistry from Research Center for Ecological Environment, Chinese Academy of Sciences, China in 2010. He is currently an professor at Beijing Center for Disease Control & Prevention, China. Researching field is target analysis of chemical hazards in environment, food and biological matrix, including toxins, pharmaceuticals and personal care products and environmental contaminants.